DEPENDENCE OF A PLANE TURBULENT JET ON ITS NOZZLE CONTRACTION PROFILE

Deo*, R C, Mi, J and Nathan, G J

School of Mechanical Engineering
The University of Adelaide
SA 5005 AUSTRALIA
*ravinesh.deo@usp.ac.fj

ABSTRACT

The present study investigates experimentally the effect of the nozzle contraction profile on the downstream development of a plane turbulent jet. The variation of the contraction profile was made by using various orifice plates with different radii. It is found that the decay and spread rates of the jet's mean velocity increase as the radius decreases. A decrease in the radius also results in a higher formation rate of the primary vortices. Moreover, the turbulence intensity is found to depend on the contraction profile.

INTRODUCTION

A half century ago, the analytical study of Batchelor and Proudman [1] provided a linear theory on a rapid distortion of a fluid in turbulent motion issuing in a round contraction. Later, Uberio [2] investigated experimentally square cross-sections of round contraction ratios 4, 9 and 16. Klein and Ramjee [3] investigated the effect of exit contraction geometry on non-isotropic free-stream turbulence. They used eight nozzles of circular cross-sections, differently contoured shapes and various non-dimensional. The influence of the axisymmetric contraction ratio on free-stream turbulence was studied more thoroughly by Ramjee and Hussain [4], with particular applications to wind tunnel designs. Unfortunately, these studies were conducted to understand the turbulence development within the initial (and upstream) region of the axisymmetric flow. No deduction about the downstream flow was made.

Thus, for round jets, the effect of the nozzle profiles has been studied well by quite a few investigations. The initial and downstream flow from a round smoothly contracting nozzle, a round sharp-edged orifice and a long pipe was explored by Mi et al. [5]. Some other investigators e.g. Antonia and Zhao [6] and Hussain and Zedan [7] have also studied a smoothly contracting nozzle and a long pipe flow. On the other hand, Hussain and Clark [8] quantified to some extent, the downstream effect of having a laminar or turbulent boundary layer at nozzle lip of a quasi-plane jet. Others, e.g. Goldschmidth and Bradshaw [9] studied the effect of initial turbulence intensity on the flow field of a plane jet. Additionally, Hussian [10] conducted a flow visualization of an initially laminar plane jet, issuing from two nozzles: (1) with a 96:1 contraction and (2) from the end of a duct attached to a contoured nozzle, and noted a dependence of the vortex formation on the nozzle profile. Thus, it is well understood that the nozzle profile does affect the downstream flow of a plane jet. However, the effect of different magnitudes of contraction has not been studied.

The present investigation is undertaken to provide an insight into the velocity field of a plane jet from nozzles of different exit contraction profiles.

EXPERIMENTAL DETAILS

The experimental set-up has been described in detail elsewhere (Deo *et al.* [11]. Briefly, the plane nozzle facility consists of an open circuit wind tunnel with flow straightening elements and a smooth contraction exit, whose dimensions are 720 mm × 340 mm. Attached to the wind tunnel exit is a plane nozzle, that consists of two perspex plates, mounted vertically but with an opening width H = 10 mm in the center, to produce a large aspect ratio plane nozzle ($AR = w/H = 72$). Sidewalls are placed in the x-y plane to enhance 2-dimensionality.

To quantify the effect of the variations in the nozzle contraction profiles on plane jets, five different sets of nozzle plates were designed and tested. Figure 1 shows the nozzle plates used for this investigation. To vary the nozzle contraction profile, r was varied systematically, for a fixed H and w, between $0 \le r/H \le 3.60$. Note that the contraction profile factor is denoted as $r^* = r/H$. Note that the configuration $r^* = 0$ (orifice-nozzle) was obtained by reversing the plates to provide a sharp 135° corner. The jet exit Reynolds number (based on slot opening width H, exit centerline mean velocity $U_{o,c}$ and kinematic viscosity of air ν, was 18,000.

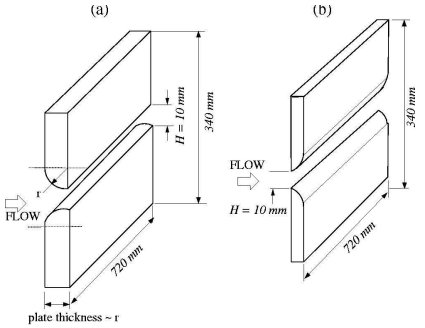

Figure 1. Nozzle plates used for exit profile variation for the cases in (a) $4.5 \le r^* \le 36$ mm, with radial contraction facing upstream and (b) radial contraction facing downstream, i.e. $r^* = 0$.

A 3-dimensional traversing system is used to undertake measurements to an accuracy of ±0.5mm. A constant temperature anemometer, in conjunction with a PC30-F data

acquisition system was employed to undertake measurements. The hot wire was calibrated in the jet potential core, where turbulence intensity was less than 0.5%. Then, the effect of nozzle exit contraction profile on the initial flow was determined by interchanging each configuration of the plate, and subsequently measuring the initial velocity profiles at $x/H = 0.25$ for $0.45 \le r^* \le 3.60$ and at $x/H = 1.25$ for $r^* = 0$. Data were sampled at *Nyquist* frequency of 18.4*kHz*, for a total duration of 22 seconds per sample. The initial velocity profiles, together with streamwise (x) distribution of the centerline velocity, the spanwise (y) distribution of the streamwise velocity were measured. The axial range of measurements used in this experiment was up to 85 nozzle widths.

RESULTS AND DISCUSSION

Figure 2a displays the lateral profiles of the normalized mean velocity at $x/H = 0.25$ for the radially contracting configurations and at $x/H = 1.25$ for the sharp-edged orifice nozzle. The downstream locations were chosen to prevent probe damage. Significantly different initial velocity profiles are evident for all nozzles due to the different exit contractions. Notably, as r^* is increased from 0 to 3.60, the normalized mean velocity profile changes from saddle-backed (for $0 \le r^* \le 0.90$) to approximately top-hat (for $r^* = 1.80$ and 3.60). Saddle-backed profiles are a characteristic of sharp-edged orifice plates (Mi et al. [5], Mi and Nathan [12]. For the saddle-backed profiles, the central `dip' is deepest for the sharp-edged orifice nozzle ($r^* = 0$ case). The local minima in the center of the saddleback are probably caused by the initial lateral contraction of the emerging fluid, termed the `vena contracta'. It also appears that the initial profiles converge for $r^* \ge 1.80$, to approximate an approximate top-hat profile. The top-hat region lies between $\xi \le 0.5$. Also, the approximate top-hat profile for $r^* \ge 1.8$ is comparable with the top-hat profiles from conventional smooth contoured nozzles e.g. Namar and Otugen [13] for a quasi-plane jet.

From Figure 2a, it appears that the thickness of the nozzle boundary layer depends on the nozzle exit contraction profile. Thus, the pseudo-boundary layer thickness δ at $x/H = 0.25$, was computed from the integral equation $\delta = \int_{y=0}^{y=\infty} \left(1 - U/U_{o,c}\right) dy$.

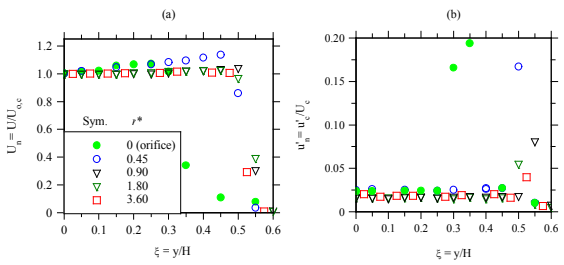

Figure 2. Lateral profiles of (a) the normalized mean velocity and (b) the turbulence intensity at the $x/H = 0.25$ for $0.45 \le r^* \le 3.6$ and $x/H = 1.25$ for $r^* = 0$.

Given the coarse measurement grid in Figure. 2a, a best-fit curve was used to perform an integration to obtain the most reliable value of δ. Figure 3 shows that as r^* is increased from 0.45 to 3.60, the pseudo-boundary layer thickness (calculated at a distance of $0.25H$ from the nozzle exit plane), becomes increases. Of course the magnitudes of δ for the sharp-edged orifice plate ($r^* = 0$) do not truly represent the pseudo-boundary layer thickness, hence was not computed from the initial velocity profiles. Ideally, a truly sharp-edged orifice-plate is expected to have a very thin boundary layer ($\delta \sim 0$). Hence, it was assumed that $\delta = 0$ for the sharp-edged orifice nozzle. Thus, the best fit curve for the calculated δ values were extrapolated to obtain the δ for $0.45 \le r^* \le 3.60$. It is found that δ increases as the nozzle exit contraction profile changes from a sharp-edged orifice to a radially contoured configuration.

Figure 2b investigates the lateral profiles of the normalized turbulence intensity at $x/H = 0.25$ for the radially contracting and at $x/H = 1.25$ for the sharp-edged orifice nozzle. Turbulence intensity in the shear layer is about 20% for the sharp-edged orifice nozzle, while for the radially contoured ($r^* = 3.60$) configuration it is only 4%. The sharp-edged orifice has a higher turbulence intensity because its initial shear layer is the thinnest, highly unstable and an initial upstream separation causes the greatest instability within the boundary layer. However, large radius contoured nozzle ($r^* \ge 1.8$) produce an initially laminar flow, with lower turbulence intensity in the shear layer. For these cases, as r^* is increased from 0.45 to 3.60, a corresponding decrease in the peak shear layer intensity (from 17% to 4%) is evident. The turbulence intensity in the central region varies between 2.8% and 1.7%. In particular, the sharp-edged orifice nozzle produces much higher central region turbulence intensity. Furthermore, identical values of core turbulence intensity are found for $r^* = 1.80$ and 3.60.

The near field normalized mean velocity on the centerline $U_{n,c} = U_c / U_{o,c}$ is presented in Figure 4a. The figure demonstrates that the decay of mean velocity is dependent on r^*. A local maximum (hump) in $U_{n,c}$ is evident at $x/H = 3$, for $0 \le r^* \le 1.80$, whose magnitude is r^* dependent.

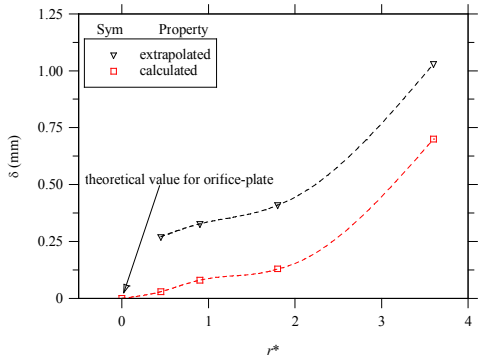

Figure 3. The calculated (at $x/H = 0.25$) and interpolated (at $x/H = 0$) pseudo boundary layer thickness δ for r^*.

This hump indicates the presence of a vena contracta. A sharp-edged orifice nozzle is known to generate a local maximum of the centerline mean velocity, as shown for example by Quinn [14]. Thus we introduce the term $U_{m,c}$ to represent the mean velocity maximum on the centerline. To assess the relative magnitudes of these local maximum for

present nozzle configurations, Figure 4b plots $U_{m,c}/U_{o,c}$ obtained at x/H = 3. As r^* is increased from 0 to 3.60, $U_{m,c}/U_{o,c}$ decreases from 1.3 to 1.0. Clearly, for the sharp-edged orifice plate, a strong vena contracta is present, with a 30% higher centerline velocity than its nominal exit centerline value. Evidently, from Figure 4b, as r $\rightarrow$ 1.8, $U_{m,c}/U_{o,c}$ asymptotes to 1 Thus this study indicates that the present nozzles with $r^* \geq 1.8$ do not produce a pronounced vena contracta.

Figure 4a also suggests that for $x/H > 6$, the centerline velocity decays faster for the sharp-edged orifice plate. Increased decay of centerline mean velocity for $x/H > 6$ for this configuration is probably a consequence of the sudden `expansion' of the jet (or possibly increased entrainment by the jet) as it emerges from the sharp-edged nozzle. Such an expansion is caused by an initial separation of the flow due to a lateral contraction of the emerging fluids. The radially contoured nozzles however, allow a more smooth flow from their exit. The radial contraction avoids a flow separation, thus producing an approximate top-hat velocity profile and a lower decay of centerline mean velocity when compared with a sharp-edged orifice plate and no vena contracta. The present observation is well supported by Mi et al. [5], who demonstrated that the decay of the centerline mean scalar field for a sharp-edged round nozzle was higher, when compared with the smoothly contoured round nozzle.

Figure 5a presents the normalized centerline velocity decay for the entire measured range. The well-known inverse square dependence of a plane jet, of the form $\left(\frac{U_{o,c}}{U_c}\right)^2 = K_u\left[\frac{x}{H} + \frac{x_{01}}{H}\right]$ is demonstrated, where K_u is the slope determined from experimental data ranging between $20 \leq x/H \leq 80$, x_{01} is the x-location of the virtual origin.

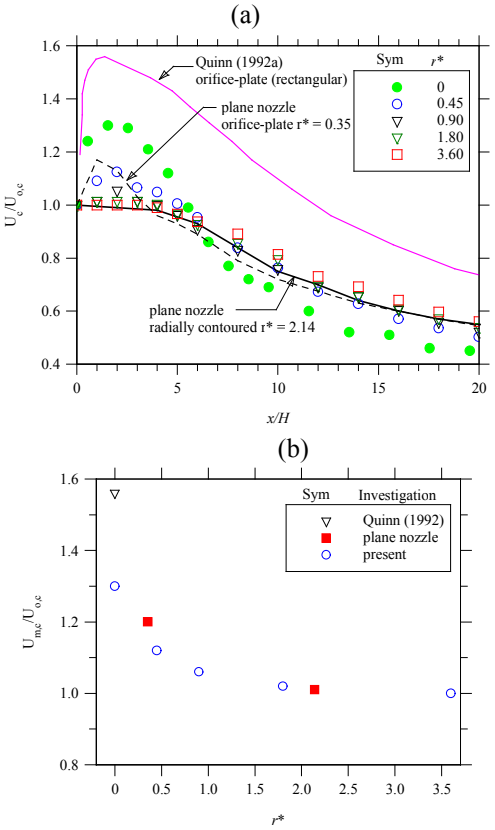

Figure 4 (a) The near field evolution of the normalized mean centerline (b) The dependence of the ratio of the centerline mean velocity maximum, $U_{m,c}$ to the exit centerline mean velocity $U_{o,c}$ on r^* at $x/H = 3$.

Heskestad's [15] orifice-jet, measured at (Re, AR) = (36,800, 120), compares relatively well with present measurements for the orifice-jet at (18,000, 72). Also, Jenkins and Goldschmidt [16], who measured a smoothly contoured nozzle at (Re, AR) = (14,000, 24) compares relatively well with our radially contoured nozzle, whose r^* = 3.60. As evident from Figure 5a, the highest decay of centerline mean velocity occurs for the jet issuing through the orifice nozzle. A collapse of $U_{n,c}$ is also noticeable for r^* = 1.80 and 3.60. Any differences between them are within the experimental uncertainty.

Figure 5b presents the relationship between r^* and K_u. As r^* is increased from 0 to 3.60, K_u decreases from 0.240 to 0.165. Consistent with Figure 5a, K_u asymptotes to a constant value for r^* = 1.80 and 3.60. Moreover, the inclusion of the K_u for Heskestad [15] and Jenkins and Goldschmidt [16], for their sharp-edged orifice and smooth contraction nozzles respectively, show a reasonable `baseline' comparison with the present magnitudes of K_u. An analysis of the virtual origins of centerline mean velocity decay, x_{01} shows that x_{01} increases monotonically with r* to x_{01} = 4.7 at r^* = 3.60. Hence, x_{01} is smallest for the sharp-edged orifice plate, with x_{01} = 2 at r^* = 0. This dependence of x_{01} on initial conditions is in agreement with the postulate of Gouldin et al. [17], who attributed the large scatter in x_{01} of plane jets with different initial conditions. The reduced magnitude of the present x_{01} for r^* = 0 is perhaps associated with the presence of a vena contracta for the sharp-edged orifice nozzle. For this case, an initial radial inflow could produce a smaller virtual `width' of the potential core.

Figure 6a presents the streamwise variations of the normalized velocity half-width $y_{0.5}/H$. (The half-widths were derived from the lateral profiles of the mean velocity, measured at selected downstream locations. Note that $y_{0.5}$ is the y-value where the mean velocity U was half of its centerline value U_c, i.e. at $y_{0.5}$, $U = \frac{1}{2}U_c$). It is clear that the present data conforms to the following self- similar relation $\frac{y_{05}}{H} = K_y\left[\frac{x}{H} + \frac{x_{02}}{H}\right]$, where K_y and x_{02} are experimental constants. As r^* is decreased from 3.60 to 0, the jets spreads at increased rates so that the greatest spreading occurs for the sharp-edged orifice nozzle. This trend is consistent with the effect of r^* on the higher decay of U_c (Figures 5). The spreading rates K_y are presented directly in Figure 6b. Again, the sharp-edged orifice nozzle has the greatest spread. Increased far-field spreading rate of the orifice is indicative of its greater entrainment of ambient fluid and probably also of increased mixing, although mixing rates cannot be determined explicitly from velocity measurements alone. On the other hand, Mi et al [5] calculated the mixing rates from an orifice plate and a smoothly contracting round nozzle. Their planar images of the scalar field showed highest mixing, decay and spreading rates for the orifice plate. Hence, we can infer to some extent, that our deduction that the orifice plate has the highest decay, spread and possibly mixing rates is somewhat justified. As demonstrated by Figure 5b, the virtual origins (x_{02}/H)

depend on r^* too. As r^* is increased from 0 to 3.60, the magnitude of x_{02}/H increases from 0 to 4 respectively. Thus, the sharp-edge orifice nozzle generates a `smaller' virtual origin when compared with a contoured nozzle.

Figure 7a demonstrates the streamwise evolution of the locally normalized turbulence intensity fields. For comparison, $u_{n,c}$ of a previous set of preliminary measurements, for the sharp edged orifice nozzle and a radially contoured nozzle at (Re, AR) = (16,500, 10) and (16,500, 60) are included. Also included are the smoothly contracting plane jet data of Gutmark and Wygnanski [18] and Heskestad [15], measured at (Re, AR) = (30,000, 39) and (36,900, 120).

Turbulence intensity also shows a significant dependence on r^*. Its dependence is the greatest in the near field, although even in the far field, asymptotic values also differ. In particular, the near field of the orifice jet is distinctly different from the radiused nozzle jet. The initial relative turbulence intensity are much higher for the orifice jet, with a major `hump' at x/H = 10. This is also supported by our previous measurement, which displays a similar shape and also the occurrence of a hump at x/H = 10, for a sharp-orifice nozzle, whose nozzle boundary was defined by (r^*, AR) = (0.35, 10).

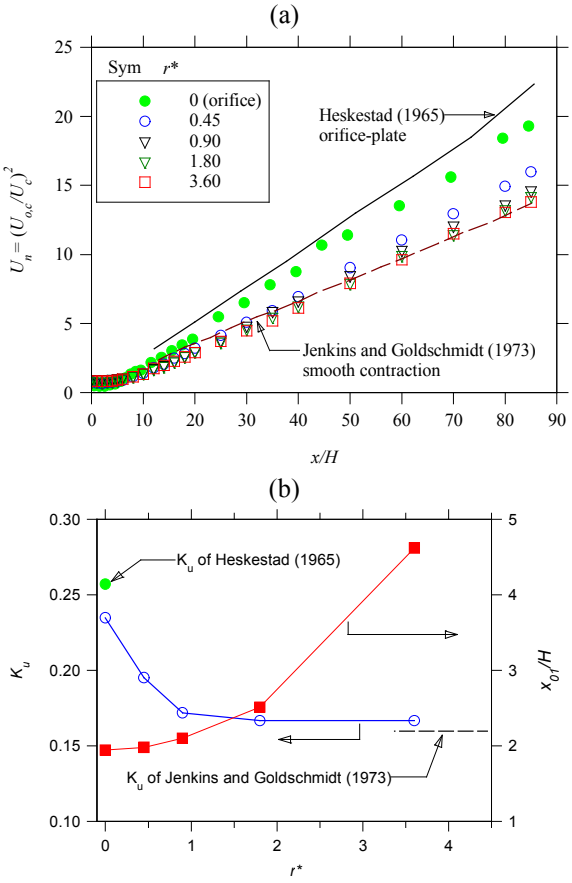

Figure 5 (a) The centerline variation of the normalized mean velocity (b) Dependence of the centerline decay rate of mean velocity, K_u and the virtual origin, x_{01} on the r^*.

The difference in intensity levels is due to the differences in the aspect ratio (10 for our previous plane jet data verses 72 for present data). The radially contoured nozzles (r^* > 0.45) do not produce a hump, except for r^* = 0.45, in which the hump is quite suppressed. Also, our previous measurements for (r^*, AR) = (2.14, 60) shows excellent comparison with present data of r^* = 1.80. Quinn [14], who measured at (Re, AR) = (36,000, 20) noted pronounced near field humps in turbulence intensity, produced by their orifice plate rectangular jet.

Hill et al. [19] has attributed the presence of the hump to initial conditions. It was deduced that the occurrence of these humps is due to the highly turbulent large-scale vortices in the interaction region (Brown et al. [20]). At this location, the centerline turbulent kinetic energy was notably higher, as envisaged by [20]. Hence, as the growing vortices move downstream from the origin to x/H = 10, the collision of vortex rings (Schultz-Grunow [21]) from both sides of the symmetric mixing layers are inevitable. This could produce much larger turbulence intensity at x/H = 10 for the sharp-edged orifice nozzle. Unfortunately, it was not possible to assess whether or not a hump was present in the sharp-edged orifice nozzle studied by Heskestad [15], at (Re, AR) = 36,900, 120). A careful check of his data shows that his measurements were mostly taken in the far field and very few points in the near field. On the other hand, the radially contoured nozzles (r^* > 0.45) produce a smoother transition of turbulence intensity, with no near field humps. Namar and Otugen's [13] smoothly contoured quasi-plane nozzle measured at (Re, AR) = (7,000, 56) did not show a discernable hump. However, a small hump in their intensity can be observed at x/H = 18, possibly due a low Reynolds number effect. The absence of the near field hump for the present radially contoured nozzles (i.e. for r^* > 0.45) is, therefore, unambiguously supported by previous investigations.

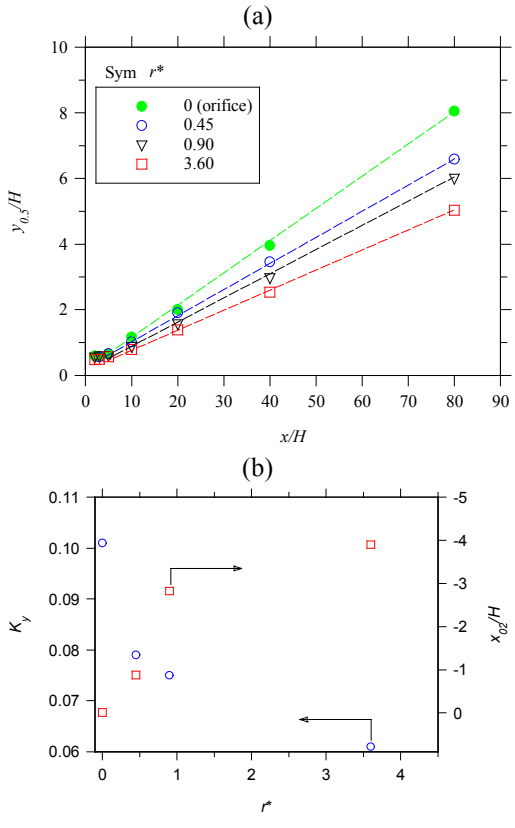

Figure 6 (a) The streamwise variation of the velocity half-width, $y_{0.5}$ (b) Dependence of the jet spreading rates, K_y and virtual origin, x_{02}/H on the r^*

The locally normalized turbulence intensity attains self-similarity at $x/H > 30$, with each reaching an asymptotic value of $u'_{c,\infty}$. The magnitude of $u'_{c,\infty}$ is plotted as a function of r^* in Figure 7b. A consistent trend is evident in the present dependence of $u'_{c,\infty}$ on r^*. As r* is increased from 0 to 3.60, $u'_{c,\infty}$ decreases from 0.28 to 0.24. This is an opposite trend to the asymptotic value of the centerline scalar intensity of a round smooth contraction and a round sharp-edged orifice nozzle (Mi et al. [22], where the intensity was smaller for the sharp-edged orifice nozzle rather than for the smoothly contoured configuration.

The reason for this possibly could be the geometric difference (planar verses circular), but cannot be stated with certainty. Furthermore, the difference in $u'_{c,\infty}$ for $r^* > 1.80$ is quite small. Also, the far field value of $u'_{c,\infty}$ of Gutmark and Wygnanski [17] conforms `closely' with $u'_{c,\infty}$ at r* = 3.60. While differences exist among the $u'_{c,\infty}$ of Bradbury [23] and that of the present ($r^* = 3.6$), these differences are probably due to different experimental conditions. For instance, [23] used a co-flow (ambient-jet-velocity ratio ~ 7-16.

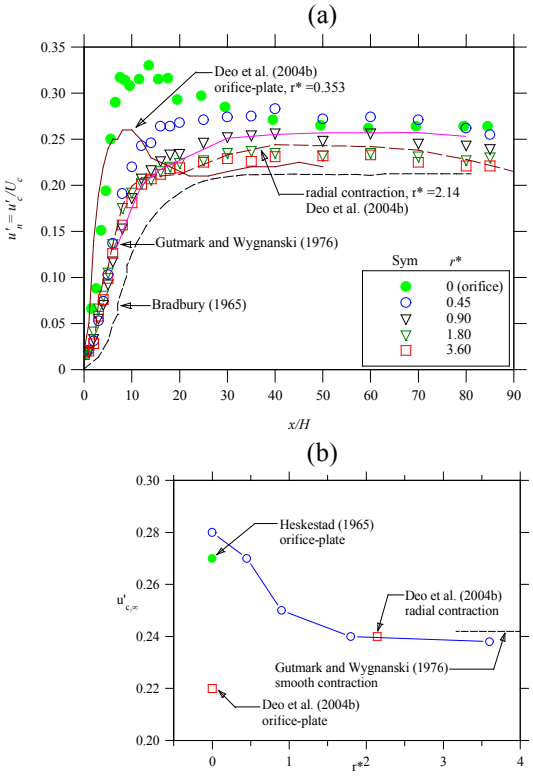

Figure 7 (a) Evolutions of the centerline turbulence intensity (b) Dependence of the far field asymptotic turbulence intensity, on r^*

The published asymptotic values of turbulence intensity of a plane jet, issuing through a sharp-edged orifice by Heskestad [15] compares extremely well with present turbulence intensity from our sharp-edged orifice nozzle. Slight differences in $u'_{c,\infty}$ are attributable to the differences in initial conditions (i.e. differences in Re, AR and geometry: refer to his paper). Further, our previous measurement from a plane jet of aspect ratio 60 (Deo et al. [11]), at (Re, r^*) = (16,500, 2.14) compares well with present results taken at r* = 1.80. However, present results at $r^* = 0$ differ from [11] at (Re, r^*) = (16,500, 0.35). This is highly likely due to the differences in nozzle aspect ratio (72 for present verses 10 for [11]. Indeed, we have shown elsewhere (Deo et al. [24]) that a reduction in nozzle aspect ratio leads to a decrease u'_c. Thus, the present data is entirely consistent with previous work.

CONCLUSIONS

Hot-wire measurements of the streamwise velocity in a plane jet, up to 85 nozzle width downstream; have been performed by varying the nozzle contraction radius over the range $0 \le r/H \le 3.60$. The objective is to examine the effect of the nozzle contraction profile on the downstream development of the turbulent plane jet. Results obtained from this study show the following:

- The initial mean velocity profile varies with the nozzle profile, r^*. This dependence propagates downstream into the whole field, leading to an increase in both the decay and spreading rates of the mean velocity field when r^* is decreased.
- The turbulence intensity, in both the near and far fields, increases as r^* decreases.
- The vena contracta occurs when $r^* \le 0.90$.

ACKNOWLEDGMENTS

This research was a major focus of the primary author's PhD in Fluid Engineering, at the University of Adelaide, accomplished through the support of ARC and IPRS, both of which are greatly acknowledged.

REFERENCES

[1] Batchelor, G. K., and Proudman, I.., The effect of rapid distortion of a fluid in turbulent motion, *Quart. J. Mech. Appl. Mech*. **7**, pp. 83-103, 1954

[2] Uberio, M S., Effect of wind tunnel contraction on free-stream turbulence, *J. Aero. Sci.* **23**, pp. 754-764, 1956

[3] Klein, A and Ramjee, V., Effect of contraction geometry on non-isotropic freestream turbulence, *Aero. Quart.* **23**, pp. 34-38, 1972

[4] Ramjee, V and Hussain, A. K. M. F., Influence of the axisymmetric contraction ratio on free-stream turbulence, *J. Fluids. Eng* **507**, pp. 506-515, 1976

[5] Mi, J., Nathan, G. J and Nobes, D. S., Mixing characteristics of axisymmetric free jets from a contoured nozzle, an orifice plate and a pipe, *J. Fluid. Eng*. **123**, pp. 878-883, 2001

[6] Antonia, R. A. and Zhao, Q., Effects of initial conditions on a circular jet, *Exp. Fluids* **31, pp.** 319-323, 2001

[7] Hussain, A. K. M. F. and Zedan, M. F., Effect of the initial conditions of the axisymmetric free shear layer: effect of initial momentum thickness, *Phys. Flu*ids, **21**, pp. 1100-1112, 1978

[8] Hussain, A. K. M. F. and Clark, A R., Upstream influence on the near field of a planar turbulent jet, Phys. Fluids **20**(9), 1977
[9] Goldschmidth, V. W. and Bradshaw, P., Effect of nozzle exit turbulence on thespreading (or widening) rate of plane free jets*, Joint Engineering, Fluid Engineering and Applied Mechanics Conference*, ASME, ASME, Boulder, Colarado, pp. 1-7, 1981
[10] Hussian, A. K. M. F., Coherent structures - reality and myth, *Phys. Fluids* **26**, pp. 2816-2850, 1983
[11] Deo R C., Mi J and Nathan G J., An Experimental Investigation on the Influence of Nozzle Aspect Ratio on the Velocity Field of a Turbulent Plane Jet, In Proc. *15th Australasian Fluid Mech. Conference,*13-17th Dec 2004, University of Sydney, Australia, 2004
[12] Mi, J and Nathan, G J., Mean Velocity Decay of Axisymmetric Turbulent Jets with Different Initial Velocity Profiles, In Proc. 4th *Int. Conf. on Fluid Mech*., July 20-23, Dalian, China, 2001
[13] Namar, I. and Otugen, M. V., Velocity measurements in a planar turbulent air jet at moderate Reynolds numbers, Exp. Fluids **6**, pp. 387-399, 1988
[14] Quinn, W. R., Turbulent free jet flows issuing from sharp-edged rectangular slots: The influence of slot aspect ratio, *Exp. Therm. Fluid Sci.,* **5**, pp. 203-215, 1992
[15] Heskestad, G., Hot-wire measurements in a plane turbulent jet*, Trans. ASME, J. Appl. Mech.* **32** pp. 721-734, 1965
[16] Jenkins, P. E. and Goldschmidt, V. W., Mean temperature and velocity measurements in a plane turbulent jet, *Trans. ASME J.* **95**, pp. 81-584, 1973
[17] Gouldin, F. C., Schefer, R. W., Johnson, S. C., Kollmann, W., Non-reacting turbulent mixing flows, *Prog. Energy Combust. Sc*, **12,** pp. 257-303, 1986
[18] Gutmark, E. and Wygnanski, I., The planar turbulent jet, *J. Fluid Mech*.73(3), 465-495, 1976
[19] Hill, W. G., Jenkins, R. C. and Gilbert, B. L., Effects of the initial boundary layer state on turbulent jet mixing, *AIAA J.* **14**, pp. 1513-1514, 1976
[20] Brown, L. W. B., Antonia, R. A., Rajagopalan, S. and Chambers, A. J., Structure of complex turbulent shear flows, IUTAM Symposium, Marcseille, pp. 411-419, 1982
[21] Schultz-Grunow, F., Generation of spatial turbulent spots, In *Proc.7th Biennial Symp. On turbulence*, University of Missouri-Rolla 52-1 to 52-4, 1981
[22] Mi, J., Nobes, D. S. and Nathan, G. J., Influence of jet exit conditions on the passive scalar field of an axisymmetric free jet, *J. Fluid Mech*. **432**, pp. 91-125, 2001
[23] Bradbury, L. J. S., The structure of self-preserving turbulent planar jet*, J. Fluid Mech.* **23**, pp. 31-64, 1965
[24] Deo, R C., *Experimental Investigation on the Influence of Reynolds Number and Boundary Conditions on the Velocity Field of a Plane Air Jet*, Ph.D. Thesis, School of Mechanical Engineering, The University of Adelaide, South Australia, May, 2005